CONVERSION OF IRRADIATED URANIUM METAL TO UO2 FOR SAFE INTERIM STORAGE AND FINAL DISPOSAL

Conference Paper · September 2019

CITATION
1

READS
257

4 authors, including:

Anders Puranen
AB SVAFO
24 PUBLICATIONS **99** CITATIONS
SEE PROFILE

Kyle Johnson
Studsvik AB
13 PUBLICATIONS **187** CITATIONS
SEE PROFILE

Alexandre Barreiro Fidalgo
Studsvik AB
15 PUBLICATIONS **70** CITATIONS
SEE PROFILE

CONVERSION OF IRRADIATED URANIUM METAL TO UO_2 FOR SAFE INTERIM STORAGE AND FINAL DISPOSAL

Anders Puranen[1], Kyle D. Johnson[1], Alexandre Barreiro[1],
Peter Bennett[2]

1) Studsvik Nuclear AB, SE-611 82 Nyköping, Sweden, anders.puranen@studsvik.com
2) Institutt for Energiteknikk, Halden, Norway.

The operation of early test reactors in the 1950s and '60s led to the creation of relatively small inventories in the range of several tons of irradiated metallic uranium fuel at a multitude of sites. Various waste management strategies have been adopted for these legacy fuels, ranging from reprocessing to extended interim storage. After several decades, some interim storage facilities have proven vulnerable to the intrusion of moisture, which is itself associated with the degradation of storage safety via oxidation and hydriding of the metallic fuel as well as the production of potentially explosive concentrations of hydrogen gas. This paper presents a new route to stabilize and facilitate disposal of metallic uranium fuels.

The Studsvik Small Scale Conversion process converts irradiated metallic U to UO_2 pellets, similar to irradiated LWR UO_2 fuel. The process thus aligns the difficult to handle metallic uranium with existing backend pathways for UO_2-based fuels. The controlled conversion to UO_2 allows for safer interim storage, in addition to making the fuel more compatible with the extensive research and final disposal pathways developed for UO_2-based fuels. The main steps of the process consist of calcination/oxidation of the U metal to U_3O_8/UO_3, compaction/pressing to suitable geometry and reduction to UO_2. In this study, the oxidation of irradiated (~6 kWd/kgU) and unirradiated metallic uranium samples was performed and the oxidation products prepared into pellet compacts. These compacts were then subjected to different thermal treatments between 600 °C and 1500 °C under inert and reducing atmospheres. Post treatment characterization by XRD was used to confirm oxide stoichiometry. Leaching tests under oxidizing conditions using simulated groundwater (10:2 NaCl:$NaHCO_3$) were also performed in order to assess the compatibility of the converted compacts with LWR fuel direct-disposal designs. Green pellets and higher oxides demonstrated poor leaching resistance, while incremental improvements were observed with pellets of increasing density. The results indicate that an oxidation conversion treatment can be successfully employed to stabilize legacy irradiated metallic uranium for continued interim storage or final disposal.

I. INTRODUCTION

Until 1967, the Norwegian research reactors JEEP I in Kjeller and Halden Boiling Water Reactor (HBWR) were using metallic, natural uranium fuel, resulting in nearly 10 tons of irradiated uranium metal. Metallic uranium fuels are thermodynamically instable in contact with water, humidity and air which leads to risks such as hydriding and hydrogen generation[1]. The potentially rapid aqueous corrosion of metallic uranium may also lead to high radionuclide release rates to the environment[1].

Current well-developed spent fuel disposal strategies include either the reprocessing and disposal of the vitrified waste or the direct disposal of UO_2-based irradiated fuels in a geological repository, such as the KBS-3 design[2] to be implemented in Sweden and Finland. Direct disposal of irradiated metallic uranium in a repository is also conceivable, although there are no known detailed plans or mature safety assessments of such a disposal route given the potentially very high corrosion rates of metallic uranium.

In order to provide safe interim storage and disposal conditions Studsvik has developed an evolved conditioning method based on calcination, the Studsvik Small Scale Conversion process. This process converts metallic uranium to uranium dioxide, UO_2, which improves the safety and simplifies further handling and interim storage. Most importantly, this also creates an opportunity to pursue integration into existing final disposal pathways for UO_2-based spent nuclear fuels. It is worth noting that while the conversion of metallic fuels to a more stable UO_2 form is required for generic compatibility with existing final disposal or prolonged interim storage designs for UO_2 spent fuels, its conversion to oxide also facilitates future handling and shipping. Furthermore, this conversion does not preclude reprocessing at a later stage, if desired.

II. CORROSION AND DISSOLUTION BEHAVIOR OF U METAL VS UO_2

Conversion of irradiated uranium metal to UO_2-form serves not only the purpose of mitigating the risks associated with handling a potentially pyrophoric material. It also yields a waste form that is more consistent with existing performance assessments for geologic disposal in a repository. The topic of expected fuel behaviours under disposal conditions is too extensive to be easily summarised, though (ref 3) gives an overview for UO_2 based fuels. Uranium metal and UO_2 are expected to behave very differently once in contact with ground water following failure of the designed barriers. Under anoxic (oxygen starved) or reducing conditions, which may be expected in a deep repository, metallic uranium corrodes at up to two orders of magnitude (100 times more) higher rate than at aerated conditions[1]. This is presumably due to the absence of the semipermeable protective outer oxide that forms under aerated conditions as well as adsorption of generated H_2 gas (forming UH_3) which further degrades the metal fuel matrix. This high rate of corrosion potentially leads to consumption of the entire metallic fuel inventory within a few years, in turn causing a concentrated release plume that can be difficult to manage in a disposal safety assessment. Conversely, the rate of dissolution of a UO_2-based waste form in anoxic water is expected to be governed by the very low solubility of tetravalent uranium at about $3x10^{-9}$ M (ref 4), resulting in expected matrix dissolution times ranging from many thousands of years, to complete inhibition of the dissolution, depending on the flow of water into the repository.

The typically more challenging condition that is generally the first step when assessing the release behavior of a waste form is the evaluation of corrosion and dissolution rates under aerated conditions. A large set of empirical evidence already exists showing that metallic uranium corrodes at high rate also in aqueous systems open to the air, such as in spent fuel ponds in which metallic uranium fuels with degraded cladding crumbled to sludge within decades[1]. Under oxic conditions UO_2 corrodes to form higher oxides such as U_3O_8 and UO_3 that are orders of magnitude more soluble than UO_2 due to the higher solubility of hexavalent uranyl, UO_2^{2+}, especially in water that contains carbonate (as in the case of typical groundwater), that effectively dissolves uranyl from the corroding surface, thereby forming soluble uranyl carbonate complexes.

III. URANIUM METAL TO DIOXIDE CONVERSION

Figure 1 outlines an overview of the conversion process. Critical parameters are:

- Minimizing fire hazards during oxidation
- Controlling the specific surface area of the product and its stoichiometry

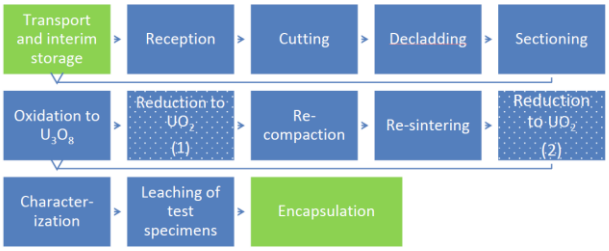

Fig. 1. Overview of the metal to dioxide conversion process.

III.A. FIRE HAZARD DURING OXIDATION

Metallic uranium is pyrophoric with its air ignition temperature depending on the surface area of the material[5]. The oxidation is also highly exothermic[6]. A maximum process temperature of 600 ˚C during the oxidation of metallic uranium was therefore chosen to provide appropriate safety margins in the case of exothermic events. Cutting was performed using a common alumina metallographic cutting blade and water coolant. From a process perspective the exothermic uranium metal oxidation is problematic, as reaction kinetics increase with increasing temperature, causing a positive feedback which complicates control of the reaction. The mechanism of reaction, the reaction kinetics, and their dependence upon reaction parameters, such as temperature, sample geometry and specific surface area, oxygen partial pressure, have been reported extensively in literature[7,8,9,10]. The progression of the reaction throughout the material is characterized by cyclic transitions between parabolic (diffusion) and linear (thermally activated) kinetics. This can be understood mechanistically by the formation of a surface oxide layer of increasing thickness, through which additional oxygen penetrates via diffusion, oxidizing residual metal below. The thickness of the formed oxide scale is generally described to be between 25-50 μm (ref 7). As this layer possesses a higher molar volume compared to the metal, stresses occur which eventually result in the spalling of this surface oxide, exposing the bare metal below. This surface metal then oxidizes according to linear kinetics, until the thickness of the oxide scale once again increases, resulting in cyclic formation of oxide scale and regeneration of fresh metallic surface, giving rise to cyclic transitions in the reaction kinetics. The practical implication of this mechanism is a process which is highly sensitive to the surface condition of the oxidizing material, as reaction kinetics – and thus the resultant heat emitted – vary considerably and rapidly during the detachment of the oxide scale. This impacts directly on the choices of furnace and control systems suitable for deployment during a process scale up. In this case, a furnace with minimal thermal insulation/inertia is preferred, such that rapid changes in heat produced

internally by the oxidation can be rejected quickly away from the system rather than contribute to a thermal excursion event. The use of a high power infrared furnace, for example, which is designed to tolerate rapid changes in temperature (>100 °C/min) is preferable to a common resistance furnace which possesses high thermal inertia and generally features a slow response (≈20°C/min). From a control perspective, the use of valves which can halt air flow and introduce an inert gas in the event of a temperature excursion, thereby suffocating the reaction and arresting the exotherm, are deemed to increase the robustness of process safety.

III.B. PRESSING, SINTERING AND REDUCTION

Pressing was performed using a 10mm internal diameter steel die, two steel punches with chamfer, and a standard desktop hydraulic press. Powders were mixed with 0.5 %wt Acrawax® lubricant and uniaxially pressed with a load of 4 tons, yielding a pressure of ≈500 MPa. Pressure was held for approximately 5 minutes before release and ejection. Green density was calculated using the measured mass and volume calculated from height and diameter, though it bears noting that this produces a slight overestimation owing to the top and bottom pellet chamfers. Percent relative density was calculated based upon theoretical densities (TD) of UO_2, U_3O_8, and UO_3. Reduction and sintering was performed with 5% H_2 in Ar at 600 to 1500 ˚C. After sintering, density was calculated using the Archimedes method, with chloroform as the immersion liquid.

IV. SCOPING TESTS ON UNIRRADIATED METAL

A series of scoping tests were performed on unirradiated uranium metal prior to the tests on irradiated uranium metal. The unirradiated material was of the same origin as the irradiated fuel, being composed of slugs of 2.54 cm diameter (1 in) and 30 cm length (12 in) of metallic uranium of natural enrichment. The unirradiated slugs had been stored in a dry environment for over 50 years resulting in an approximately 10 µm thick oxide layer. Portions of the unirradiated material were sectioned by a diamond cutting wheel using water coolant with no visible sparks observed. The samples were oxidized in a vertical furnace with a controlled flow of dry technical air. The arrangement was such that the oxide could spall off and be collected. Post oxidation X-ray diffraction (XRD, Malvern Panalytical X'pert) determined the product to be a mixture of orthorhombic U_3O_8 and orthorhombic UO_3, with no residual metal.

The evolution of sintered density relative to sintering temperature can be seen in Figure 2, where treatments between 1000 °C and 1500 °C yielded densities between 78 %TD and 90 %TD based upon a UO_2 product. The fraction of open porosity in the material was also observed to decrease; from 67 % after the 1000 °C treatment down to 56 % after 1500 °C. Perhaps unintuitively, the %TD of pellet SM-6 actually decreased during treatment while its real density increased slightly, which can be explained by the higher density of UO_2 compared to U_3O_8.

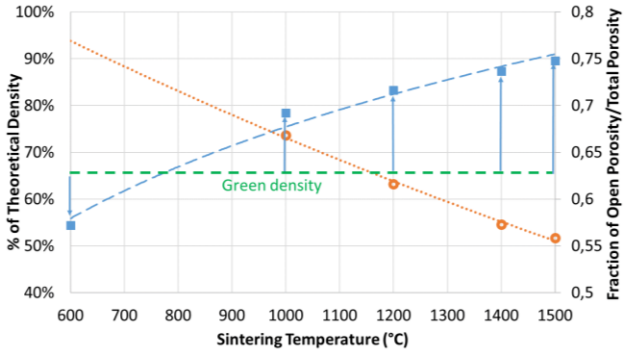

Fig. 2. Effect of Sintering Temperature on sintered density (dashed blue line and square symbols) and fraction of open porosity (dotted orange and open circles).

Following sintering, the pellets were then sliced into approximately two sections of 1:2 length. The smaller portion was reserved for characterization and the larger subjected to leaching experimentation. X-ray diffraction was performed on the internal portion of the sliced samples to provide a measurement of the bulk material.

Rietveld analysis was performed for each diffraction pattern in order to obtain an accurate lattice parameter determination. From the lattice parameter, it is possible to infer oxide stoichiometry, as the inclusion of additional oxygen atoms in UO_2 causes a known matrix contraction, and hence reduction in the overall lattice parameter. The calculated lattice parameters and inferred stoichiometries for these samples can be found in Table 1.

TABLE I. Calculated Lattice parameter (Å) and inferred stoichiometry

Sample	Lattice Parameter (Å)	Inferred Stoichiometry (UO_x)
SM6 (Pressed UO_2)	5.469	2.02±0.01
SM7 (Sintered 1000°C)	5.471	2.00±0.01
SM8 (Sintered 1200°C)	5.471	2.00±0.01
SM9 (Sintered 1400°C)	5.472	2.00±0.01
SM10 (Sintered 1500°C)	5.471	2.00±0.01
SM11 (Reduced 600°C)	5.463	2.08±0.01

For samples SM7 to SM10, Rietveld analysis revealed a lattice parameter consistent with stoichiometric $UO_{2.00}$, whereas the parameters obtained for SM-6 and SM-11 yielded slightly to moderately hyperstoichiometric UO_{2+x}, respectively. This indicates that higher

temperatures (≥1000 °C) will likely be necessary in the final process, even if only to ensure reduction to $UO_{2.00}$.

V. TESTING ON IRRADIATED URANIUM METAL

A section of irradiated uranium metal from the JEEP I reactor was transported from the hot cell laboratory of Institutt for Energiteknikk (IFE) in Kjeller, Norway to the hot cell laboratory of Studsvik Nuclear in Sweden. The sample had undergone post irradiation examinations (PIE) at Kjeller[11] including polishing for metallographic examinations. The specimen consisted of the aluminium cladding and the metallic uranium fuel. A notable feature is the uranium hydride blister visible in the upper part of the fuel-to-clad interface in Figure 3.

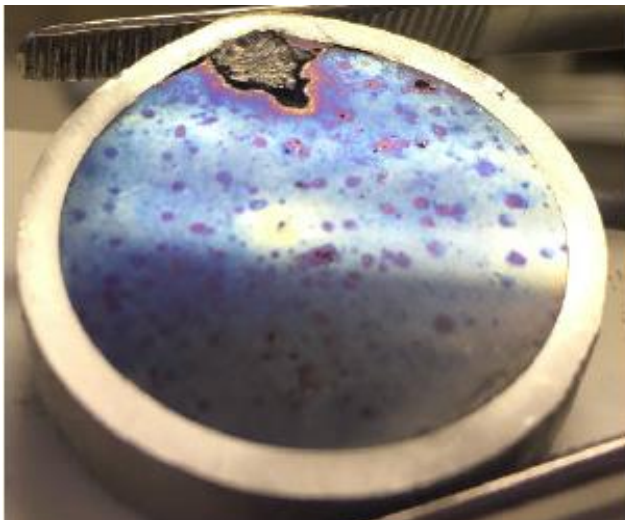

Fig. 3. Irradiated metallic uranium fuel sample with hydride blister and its aluminium cladding.

The uranium metal was easily separated from the cladding after the cladding was cut. The uranium hydride blister detached from the uranium metal, adhering instead to the clad. Since the sample had been prepared and subjected to PIE[11] in 2012 at Kjeller, it was of interest to study if the blister still consisted of uranium hydride after over 6 years of handling and storage in air. The blister was fairly hard and had a mineral appearance, and was firmly adhered to the inside of the cladding. To obtain material for X-ray diffraction, the blister was scraped with a scalpel. This scraping resulted in sparks, ignition and brief burning of the material, Figure 4, itself an indication of significant quantities of residual UH_3. XRD with Rietveld refinement confirmed the presence of uranium hydride, yielding a composition of approximately 60 % $UO_{2.12}$ and 40 % UH_3 even after ignition during sample preparation. No residual metal could be discerned by diffraction.

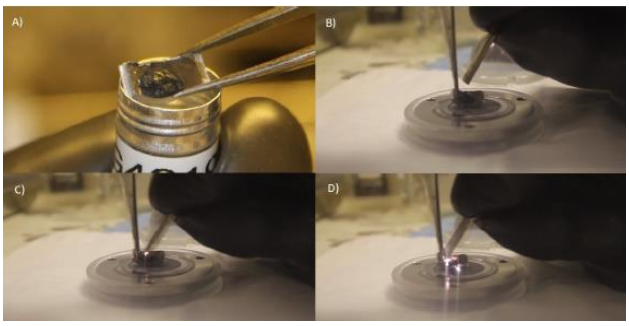

Fig. 4. A) View of hydride blister bonded to Al-clad, yielding a generally mineral appearance, B) view of blister before mechanical fretting, C) view of first sparks during mechanical fretting, D) view of sparking at both point of mechanical fretting as well as flashing of liberated UH_3 on diffraction plate.

The uranium hydride findings are in good agreement with a recent review paper[12] on uranium corrosion by hydrogen and formation of uranium hydride . The review study confirms the stability of uranium hydrides in air, owing to a thin (<50 nm) protective oxide layer. The review[12] also states that if the hydride surface area is low enough the protective oxide prevents a pyrophoric excursion from progressing, as was observed in the ignition but non-sustained (i.e. incomplete) burning during sample preparation. The thin protective oxide layer tends to protect bulk material from isolated, sharp events, such as was observed by scraping via scalpel. This also highlights the danger of macroscopic events disturbing a larger affected area, such that can occur during handling or accident scenarios, where significant amounts of energy can be released over a larger area. Such events could thereby cause conflagration of a larger mass, if available oxidants are not suppressed, complicating the handling of large quantities of defective fuel.

The irradiated metallic uranium fuel was placed on a stainless mesh support with a thermocouple and loaded into a quartz tube in a vertical infrared furnace inside a hot cell. A flow of dry technical air (excess air flow not reaction limiting) was admitted. The sample was heated at 5 ˚C/min with constant temperature regimes of 2 hours each at 425 and 450 ˚C. The IR-furnace was shut down overnight. Following inspection and gentle shaking, a final exposure of 2 hours at 500 ˚C was performed the next day. Excellent temperature control was achieved with the IR-furnace throttling its output to follow the cyclic oxidation behavior avoiding any temperature excursions. At no time was the set point temperature exceeded by more than 5 ˚C. The bottom of the quartz tube was connected to a collection vessel. The material, consisting of flakes and powder, Figure 5, was retrieved and weighed. The mass gain resulted in a uranium oxide stoichiometry of $UO_{1.9}$, indicating either a small quantity of residual metallic U or the loss of a small quantity of

material during processing. Sampling of both powder and agglomerate/flakes for XRD was performed.

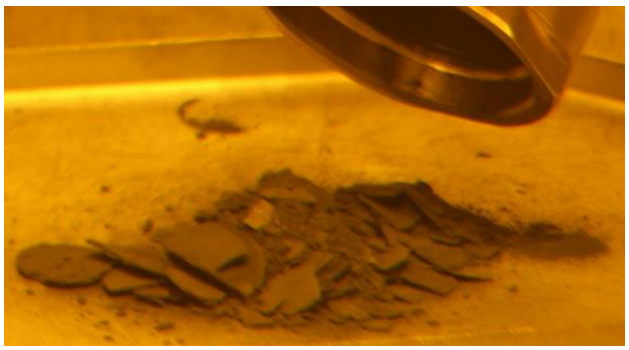

Fig. 5. Oxidised material after treatment in IR-furnace.

A second oxidation treatment was performed in a separate, horizontal tubular furnace (500 ˚C, 4 hours) in air to ensure complete oxidation of the material. A portion of the material was mixed with lubricant (Acrawax® 0.5 %-wt) and two pellets (A and B) pressed. Pellet B was reduced at 600 ˚C in 5 % H_2 in Argon (16 hours). Pellet A was sintered in argon to 1000 ˚C (4 hours) followed by reduction in 5 % H_2 in argon (4 hours).

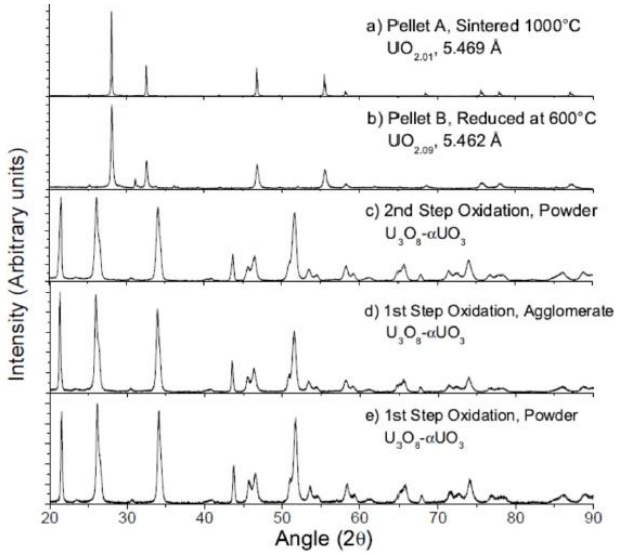

Fig. 6. X-ray diffraction spectra irradiated pellets A/B (a/b) following sintering/reduction, and oxidation products after oxidation treatment (c-e).

Figure 6 shows the XRD spectra of oxidation products and the two pellets after sintering/reduction. The oxidised products are all mainly composed of U_3O_8 and UO_3. Pellet A and B are composed of UO_2. Pellet A yielded a lattice parameter (5.4694 Å) indicating an inferred stoichiometry of $UO_{2.01\pm0.01}$ whereas pellet B (5.4625 Å) resulted in $UO_{2.09\pm0.01}$, both of which are highly consistent with their respective unirradiated analogues (Table 1).

VI. LEACHING OF UNIRRADIATED AND IRRADIATED SAMPLES

Leaching tests under oxidizing conditions using simulated granitic groundwater (10:2 NaCl:$NaHCO_3$) were performed in order to assess the compatibility of the converted compacts with LWR fuel direct disposal designs. As was outlined in section II, performing the tests in aerated carbonate water presents a conservative case for assessing the performance of a UO_2 based system, compared to the more benign case of anoxic conditions.

Figure 7, left show pellet A (2.29 g U, sintered at 1000 C˚) and, right pellet B (2.18 g U, 600 C˚ reduced) in their leaching flasks (230 ml, 10 mM NaCl, 2 mM $NaHCO_3$). All scoping test were performed with similar fuel weights, solution volumes and flasks.

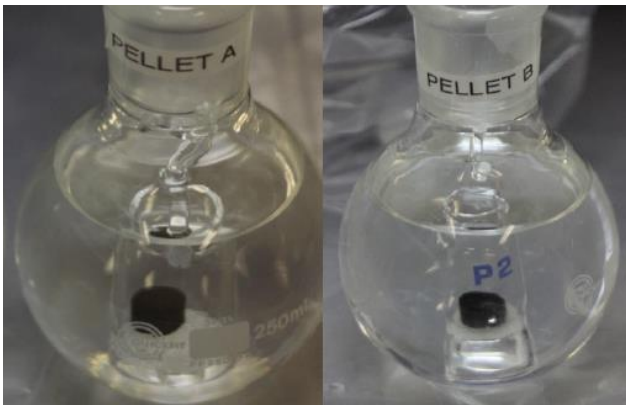

Fig. 7. Pellet A, left and pellet B, right, in their leaching flasks.

Aliquots of sampled solutions from the irradiated pellets A and B were centrifuged for one hour at a relative centrifugal force of 74 000 g just after sampling. Aliquots were also analyzed without centrifugation to assess potential colloid formation. The centrifugation did not yield any difference. Analysis of the irradiated samples was performed both by inductively coupled plasma optical emission spectrometry (ICP-OES) and inductively coupled plasma mass spectrometry (ICP-MS) whereas the uranium concentration for the unirradiated samples was analysed by UV-VIS (Arsenazo-III method) and ICP-OES.

Figure 8 presents the uranium fraction of inventory in aqueous phase (FIAP) values from both the scoping tests on unirradiated samples and of the irradiated material. The results are very consistent; the unirradiated pressed U_3O_8 pellet show comparatively high release, as is expected due to high surface area (only pressed, no sintering) and most importantly the high U oxidation state. All other samples pass the provisional benchmark criterion of less than $1x10^{-3}$ U FIAP at 30 days (<0.1% of the inventory released).

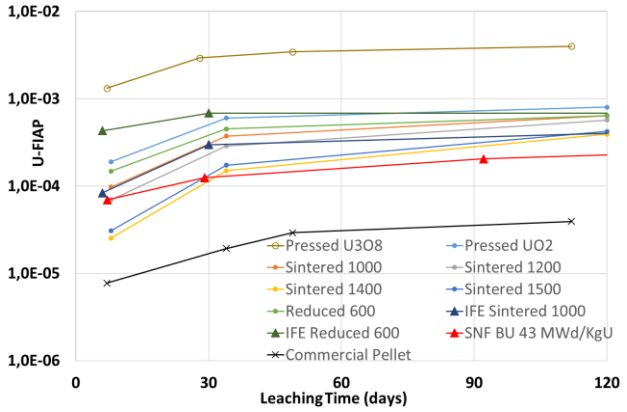

Fig. 8. U Fraction of Inventory in Aqueous phase results.

That is that less than 0.1 % of the fuel matrix is dissolved in the first 30 days of leaching. The initial 30 days typically displays the highest release rates. The 0.1% 30 day FIAP limit approximately corresponds to the expected behavior of slightly damaged regular UO_2 light water reactor fuel. The irradiated pellet B (IFE Reduced 600 in figure 8) show a comparatively low margin, presumably due to the hyperstoichiometry inferred by XRD ($UO_{2.09}$), in combination with a high surface area (no sintering). The pressed UO_2 pellet likely have the highest open porosity of the UO_2 materials with the other samples showing improved performance with higher sintering temperatures. Pellet A (IFE sintered 1000 in Figure 8) behaves very similarly to its unirradiated twin sample which is consistent with the stoichiometry inferred from XRD on the samples. As a comparison leaching results[13] under the same conditions for a power reactor UO_2 pellet with a burnup of 43 MWd/kgU are included (SNF BU 43 MWd/kgU in figure 8). Lastly leaching results from a pristine commercial as-fabricated UO_2 pellet shows superior leaching performance (Commercial pellet in Figure 8), which is to be expected given that it was sintered at the highest temperature and within a perfected industrial process, yielding a product of high density and no open porosity. Fission products and higher actinides were also measured by ICP-MS (mass range 82-254) for the irradiated samples. Given the exceedingly low burnup of only approximately 6.5 MWd/tU (0.0065 MWd/kgU) of the received irradiated sample it proved difficult to evaluate any other isotopes than U as released fractions of inventory. The release behavior of the uranium matrix and the radionuclides in the uranium decay chain are nevertheless likely to dominate the long-term safety case for these very low burnup fuels. Future studies are in the planning on samples with higher burnup to allow assessment also of elements other than the bulk uranium.

VII. CONCLUSIONS

The method appears feasible for stabilizing legacy irradiated metallic uranium for interim storage and final disposal. Further studies are underway concerning scale up, automation and optimization of the process. The method is also foreseen to have potential for conversion of other irradiated non UO_2 fuels (such as uranium silicides or nitrides) in order to make them compatible with existing disposal pathways for UO_2 fuels.

ACKNOWLEDGMENTS

The Institutt For Energiteknikk (IFE), Norway is acknowledged for financial support.

REFERENCES

1. C. H. Delegard, A. J. Schmidt. Uranium Metal Reaction Behavior in Water, Sludge, and Grout Matrices. US-DOE, PNNL-17815. 2008
2. Svensk Kärnbränslehantering AB. Utvecklingen av KBS-3-metoden SKB Report R-10-40, 2010
3. R. C. Ewing, Long-term storage of spent nuclear fuel. Nature Materials, 14, 252-257, 2015
4. R. Guillamont et al., Update on the chemical thermodynamics of U, Np, Pu, Am and Tc, OECD NEA, Elsevier 2003
5. A. L. West, Uranium Metal to Oxide Conversion by Air Oxidation–Process Development. SRNL, 2005.
6. Materialsproject.org
7. B. A. Hilton, Review of Oxidation Rates of DOE Spent Nuclear Fuel: Part I: Metallic Fuel. Oak Ridge, TN: US DOE, 2000.
8. R. J. Pearce, A Review of the Rates of Reaction of Unirradiated Uranium in Gaseous Atmospheres. UK, Central Electricity Generating Board, 1989.
9. L. Leibowitz, The Kinetics of the Oxidation of Uranium Between 125 and 250 C. 62. Journal of the Electrochemical Society, 1961, Vol. 108.
10. A. G. Ritchie, Review of the Rates of Reaction of Uranium with Oxygen and Water Vapour at Temperatures Up to 300 C. Journal of Nuclear Materials, 1981, Vol. 10
11. Investigation of one fuel element from JEEP I 1st charge from 1951. IFE report IFE/KR/F-2012/111
12. A. Banos et al. A review of uranium corrosion by hydrogen and the formation of uranium hydride. Corrosion Science, 136, 129-147, 2018
13. R. Forsyth. The SKB Spent Fuel Corrosion Programme. An evaluation of results from the experimental programme performed in the Studsvik Hot Cell Laboratory SKB Technical Report TR 97-25